

EFFECTS OF HEAT TREATMENT CONDITIONS ON MICROSTRUCTURE AND MECHANICAL PROPERTIES OF AISI 420 STEEL

C.J. Scheuer^{a,b}, R.A. Fraga^a, R.P. Cardoso^a, S.F. Brunatto^a

^a Plasma Assisted Manufacturing Technology & Powder Metallurgy Group, *Departamento de Engenharia Mecânica*, UFPR, 81531-990, Curitiba, PR, Brazil

^b *Colégio Técnico Industrial de Santa Maria*, UFSM, 97105-900, Santa Maria, RS, Brazil

ABSTRACT

The cycle control of heat treatments, on the quenching and tempering operation of AISI 420 stainless steel, is essential for improved material performance. The adequate choice of heat treatment parameters, can lead an optimization on its mechanical properties and corrosion resistance. Thus, this paper aims to investigate the effects of quenchants medium, and austenitizing and tempering temperatures, on the microstructure and mechanical properties of AISI 420 steel. Different heat treatments cycles were studied: 1) samples were austenitized at 1050°C and water, oil and air quenched; 2) samples were austenitized at range temperatures of 950-1050°C and oil quenched; and 3) as-quenched samples were tempering at range temperatures of 400-500°C. Treated samples were characterized by optical microscopy, X-ray diffractometry and hardness measurements. The samples hardness increases with increasing cooling rate (water > oil > air quenched). Water quenched samples presented crack after cooling to room temperature. Samples hardness also increases with austenitizing temperature increasing, and decreases with increasing tempering temperature.

Key-words: Heat treatment, AISI 420 steel, microstructure, mechanical properties.

INTRODUCTION

Martensitic stainless steels (MSS) containing 13% Cr are commonly used in the as-quenched and quenched-and-tempered conditions ^(1,2). In the annealed condition (as received), the MSS microstructure consist of a ferritic matrix containing spheroidized carbides ⁽³⁾. The quenching heat treatment of these steel grade (starting from the as received microstructure), involves heating to above 950 °C temperatures to obtain an austenite structure and to dissolve the carbides, followed by rapid cooling to transform the austenite into martensite structure ⁽⁴⁻

5). The material properties after heat treatment (quenching and tempering) are strongly influenced by the employees treatment parameters and, considering that material is metallurgically complex ⁽⁶⁾, the meticulous control of these parameters is necessary to obtained a fully martensitic structure without forming ferrite and retained austenite (to be avoided). Furthermore, the carbides precipitates in the quenched and quenched-and-tempered microstructures also exert effects on the material properties (hardness, wear and corrosion resistance) ^(5,7).

Thus, the aiming of this study was investigated the effects of heat treatment parameters on microstructure and mechanical properties of AISI 420 martensitic stainless steel.

EXPERIMENTAL PROCEDURE

Cylindrical samples of 10 mm in height and 9.5 mm in diameter were cut from AISI 420 steel commercial rod (composition obtained by X-ray fluorescence: 0.17% C, 0.70% Mn, 0.50% Si, 12.2% Cr, 0.23% P, 0.03% S, and Fe balance, in wt.%). Figure 1 show the material microstructure in the annealed state (as supplied). It can be noted that consists of a ferritic matrix with a homogeneous dispersion of $M_{23}C_6$ spheroidized carbides, as expected from the phase equilibrium ⁽⁸⁾. The material average hardness is 327 ± 13 HV_{0.3}.

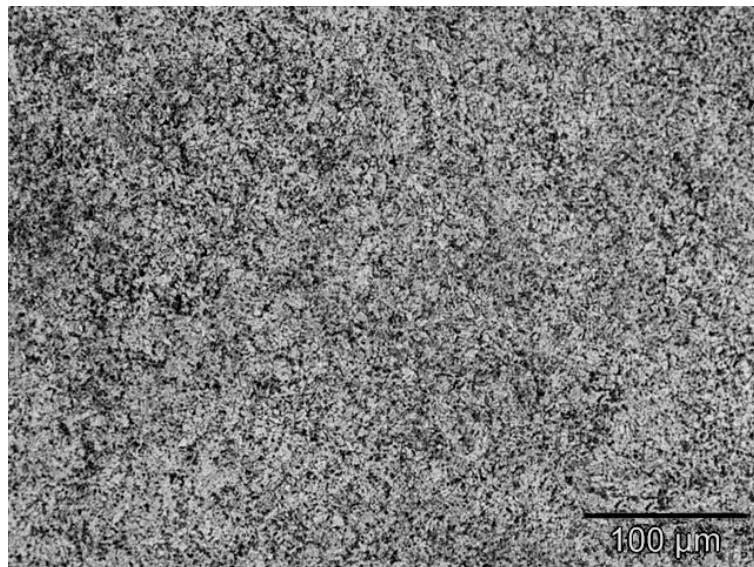


Figure 1. Microstructure of AISI 420 steel in the annealed condition.

Erro! Fonte de referência não encontrada. shows the material X-ray diffraction pattern in the annealed condition, which shows the presence of highest intensity peaks related

to α -Fe (alpha phase, ferrite). Low intensity peaks related to carbides phases are observed with an enlargement of the XRD spectrum, as shown in Figure 2 detail. These peaks can be indexed as $M_{23}C_6$ carbides, which as aforementioned, are dispersed in the ferritic matrix.

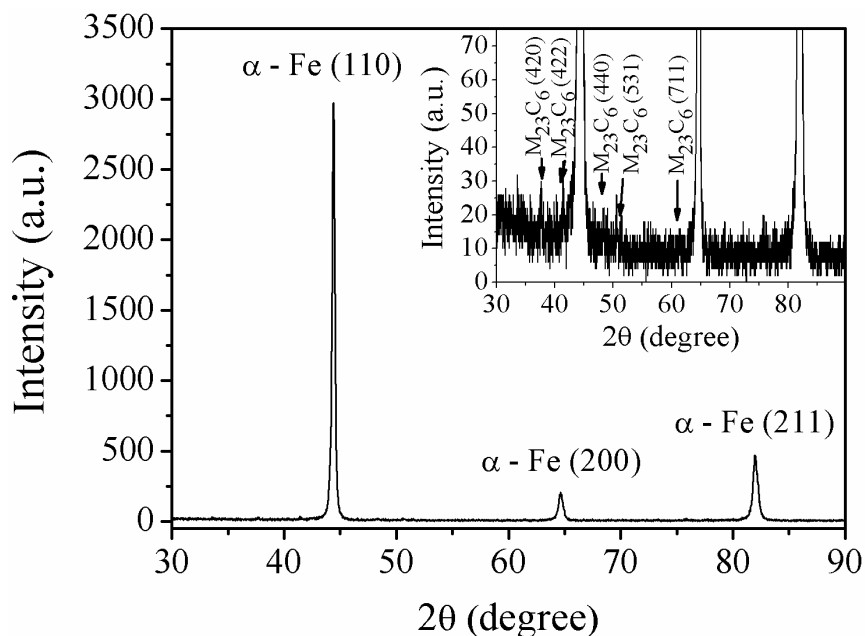


Figure 2. X-ray diffraction pattern of AISI 420 steel in the annealed condition.

To the heat treatments perform, a EDG 10P-S vacuum furnace was employed. Three different heat treatment cycles were studied: 1) samples were austenitized at 1050 °C for 0.5 h and water, oil and air quenched (cooling rate compared to water: oil 0.36 and 0.0152); 2) samples were austenitized at range temperatures of 950-1050 °C for 0.5 h and oil quenched; and 3) as-quenched samples were tempering at range temperatures of 400-500 °C for 1 h. In all treatments, a heating rate of 7°C was adopted.

Microstructure of the heat treated samples was obtained by conventional metallographic procedure. After polishing, the cross-sectioned samples were etched using Aqua regia reagent ($HNO_3 + 3 HCl$). Samples were analyzed by optical microscopy, using an Olympus BX51M microscope. The determination of the phases present in the treated samples was carried out by X-ray diffractometry (XRD) technique, using a Shimadzu XDR7000 X-ray diffractometer with a $Cu K\alpha$ X-ray tube in the Bragg–Brentano configuration, for a scan speed of 1 °/min. Hardness measurements were performed using a Shimadzu Micro Hardness Tester HVM2 T, applying a load of 300 gf for a peak-load contact of 15 s. Each point of the profile corresponds to the mean value of five indentations.

RESULTS AND DISCUSSION

1) Samples austenitized at 1050 °C and water, oil and air quenched

The influence of the quenchants medium on material hardness is shown on Figure 3. The hardness increases with the increasing cooling rate. Water, oil and air quenched samples present hardness of 569 ± 11 , 510 ± 11 and 488 ± 12 HV_{0.3}. When compared to the starting condition (as supplied), the hardness increase is a consequence of the M₂₃C₆ carbide dissolution that increases the carbon supersaturation and the lattice residual stress of the martensite^(4,5). It is assumed that the faster the cooling rate from the austenitizing to the room temperature, greater is the carbides dissolution.

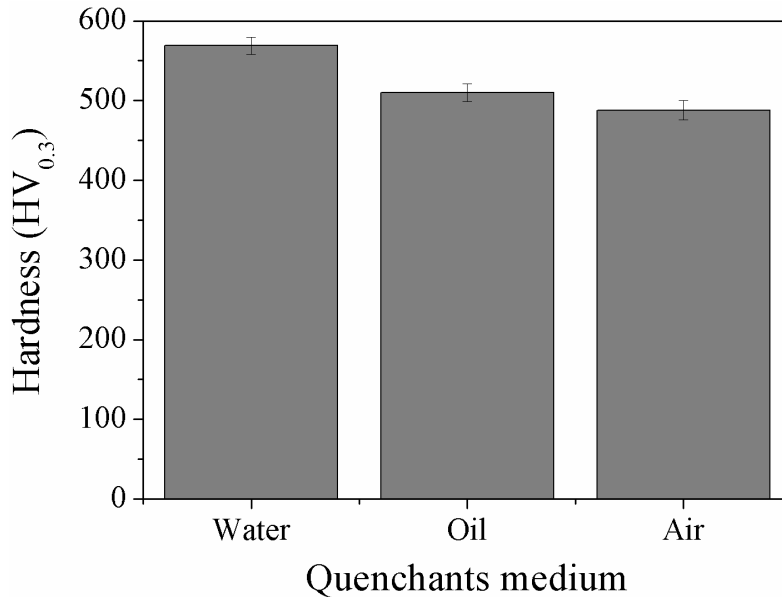


Figure 3. Effect of quenchants medium on the AISI 420 steel hardness. Samples austenitized at 1050 °C for 0.5 h and water (a), oil (b) and air (c) quenched.

Figure 4 present the XRD pattern of the samples quenched in air, water and oil quenched medium. Comparing the quenched sample diffraction patterns with the annealed ones, it is noted that for the quenched samples the XRD data present a reduction in intensity associated with a displacement to smaller angles. This result is a indicative of the heightened tension state existing in the body-centered tetragonal (BCT) structure compared to the body-centered cubic (BCC). Likewise, it can be seen that the XRD spectrum of the water quenched sample has a larger shift to the small angle compared to the oil quenched sample, and this, a biggest displaced compared to sample quenched in air. This result reflects the higher voltage generated in TCC cell due to the higher cooling rate promoted on the quenched held (in that order) in water, oil and air.

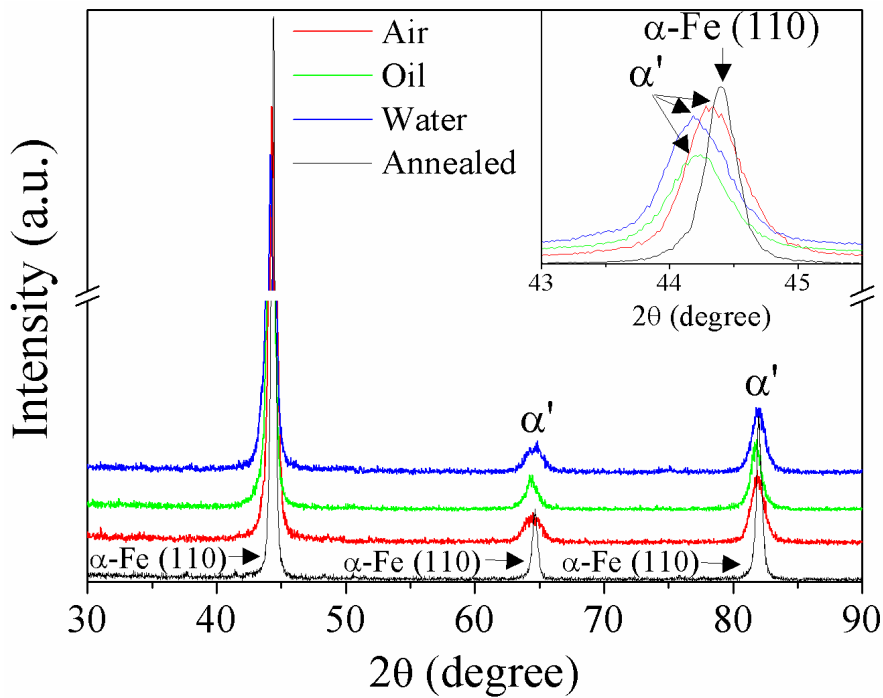


Figure 4. XRD patterns of AISI 420 steel samples cooled at different quenchants medium. Samples austenitized at 1050 °C for 0.5 h and water, oil and air quenched.

Figure 5 shows the micrograph of samples quenched at different quenchants medium. It is noted that a microstructure consisting of a martensitic matrix. The dark spots correspond to the localized corrosion attack, forming small pits with a uniform density for the three evaluated conditions. Likewise, it can be verify the crack occurrence in the water quenched sample (Figure 5(a)). In this case, the crack occurrence possibly was due to the high cooling rate, promoting a residual stress higher to the material fracture stress.

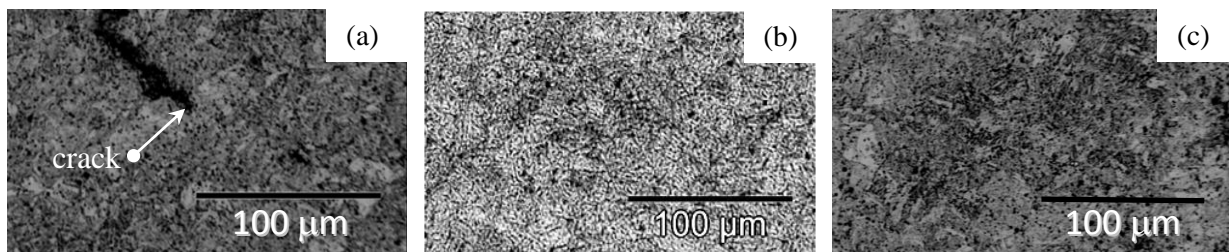


Figure 5. Microstructure of AISI 420 steel samples cooled at different quenchants medium. Samples austenitized at 1050 °C for 0.5 h and water (a), oil (b) and air (c) quenched.

2) Samples austenitized at range temperatures of 950-1050 °C and oil quenched

Figure 6 shows the effect of austenitizing temperature on the AISI 420 steel hardness. The high hardness is due to the homogenous distribution of lath martensite in the material microstructure⁽⁶⁾. According to^(5,6,9), the hardness increase with increasing austenitizing temperature can be attributed to increment of both chromium and carbon content dissolved in the martensite, due to dissolution of chromium carbides, resulting in increasing of the martensite lattice supersaturation. Candelária and Pinedo⁽⁷⁾ studied the influence of heat treatments temperatures above 1050 °C and found that from 1100 °C the material hardness decrease, due the retained austenite fraction formed from these temperatures.

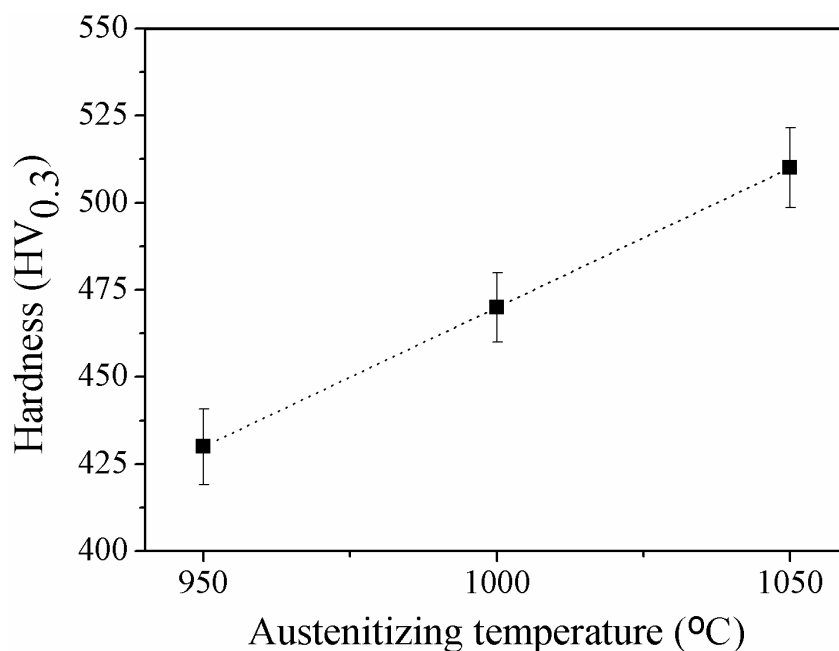


Figure 6. Effect of austenitizing temperature on the AISI 420 steel hardness. Samples austenitized at 950 (a), 1000 (b) and 1050 °C (c) for 0.5 h and oil quenched.

The XRD patterns for samples austenitized at temperatures of 950, 1000 and 1050 °C and for the material in the annealed condition are presented in Figure 7. Comparing again the annealed (α -Fe) and austenitizing (α') sample XRD spectra, it clearly appears the peaks expansion and displacement, which is due to the stress state of the martensitic lattice because its carbon saturation. With the magnification of the XRD spectrum (detail shown in Figure 7), it can be noted that the peak displacement increases with increasing quenched temperature, showing the greater chromium carbides decomposition with temperature and the increased martensite saturation by carbon.

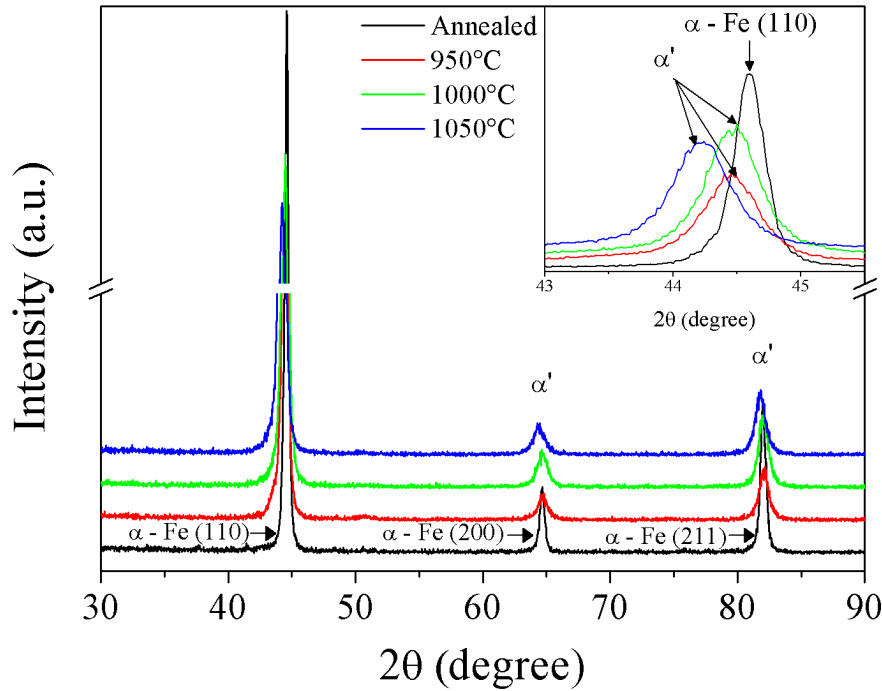


Figure 7. XRD patterns of AISI 420 steel samples austenitized at 950, 1000 and 1050 °C for 0.5 h and oil quenched.

In Figure 8 the micrographs of samples quenched at different temperatures are presented. It consists of a martensitic matrix with dispersed dark spots. As aforementioned, the dark spots correspond to localized corrosion attack. As can be seen into AISI 420 martensitic stainless steel pseudo binary equilibrium diagram, for these austenitizing temperatures, the carbides phases present in the microstructure are not totally solubilized during the heat treatment⁽⁴⁾. However, it is noted that the amount of carbides decreased with increasing the austenitizing temperature.

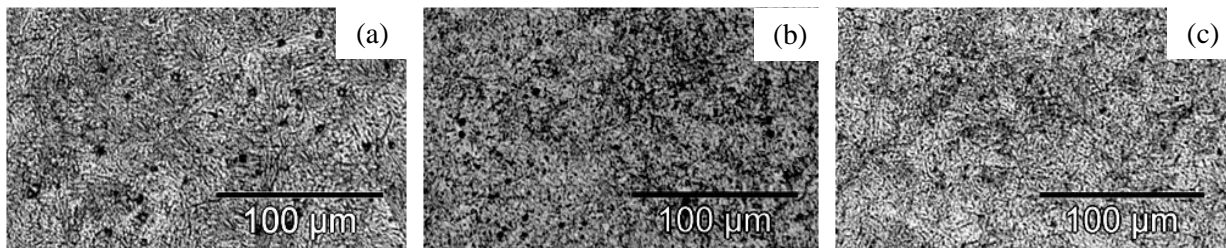


Figure 8. Microstructure of AISI 420 steel samples austenitized at 950 (a), 1000 (b) and 1050 °C (c) for 0.5 h and oil quenched.

3) Samples austenitized at range temperatures of 950-1050 °C and tempering at range temperatures of 400-500 °C

The microhardness obtained after AISI 420 steel tempering is presented in Figure 9. It can be verify a similar behavior of the hardness curves generated, which show a decrease in the material hardness with increasing tempering temperature in the studied range. This material microhardness decrease occurs due to the super-tempering effect and due to carbide precipitation ⁽¹⁰⁾.

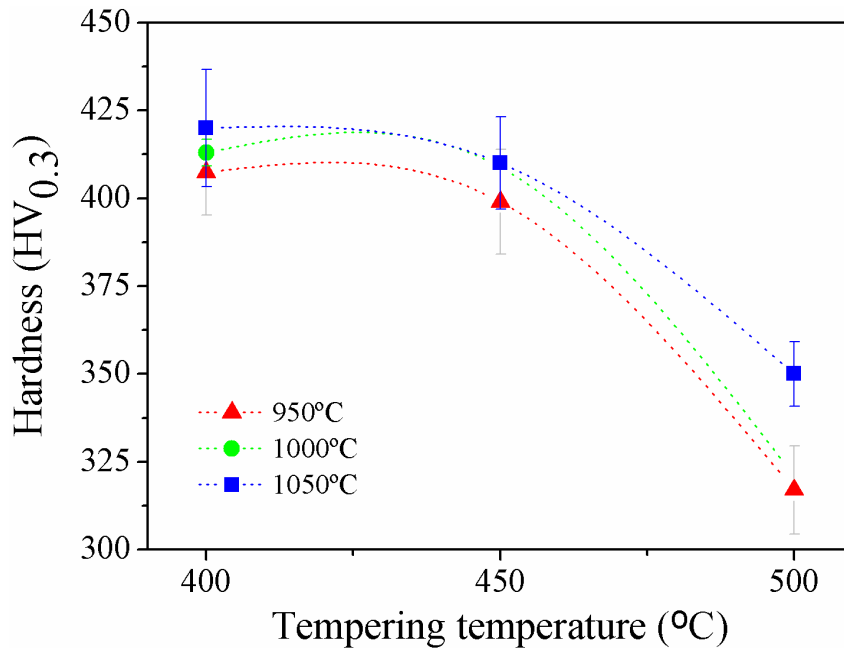


Figure 9. Effect of tempering temperature on the AISI 420 steel hardness. Samples tempered at 400 (a), 450 (b) and 500 °C (c) for 1 h.

The comparisons between the XRD data from the 400 to 500 °C tempered samples are showed in the Figure 10. Through the Figure 10(a-c) it can be seen that the XRD patterns of tempered samples show a broadening and shift to the left side, compared to the annealed samples (this can be best viewed by XRD spectrum expanding for the range of angles between 43 to 46 ° presented on Figure 10 detail.). However, by comparing them with the quenched condition spectra, visualizes that they move to the right if approximate of the initial state (annealed). This is related to the martensite tempering effect, which promotes the lattice residual stresses reduction.

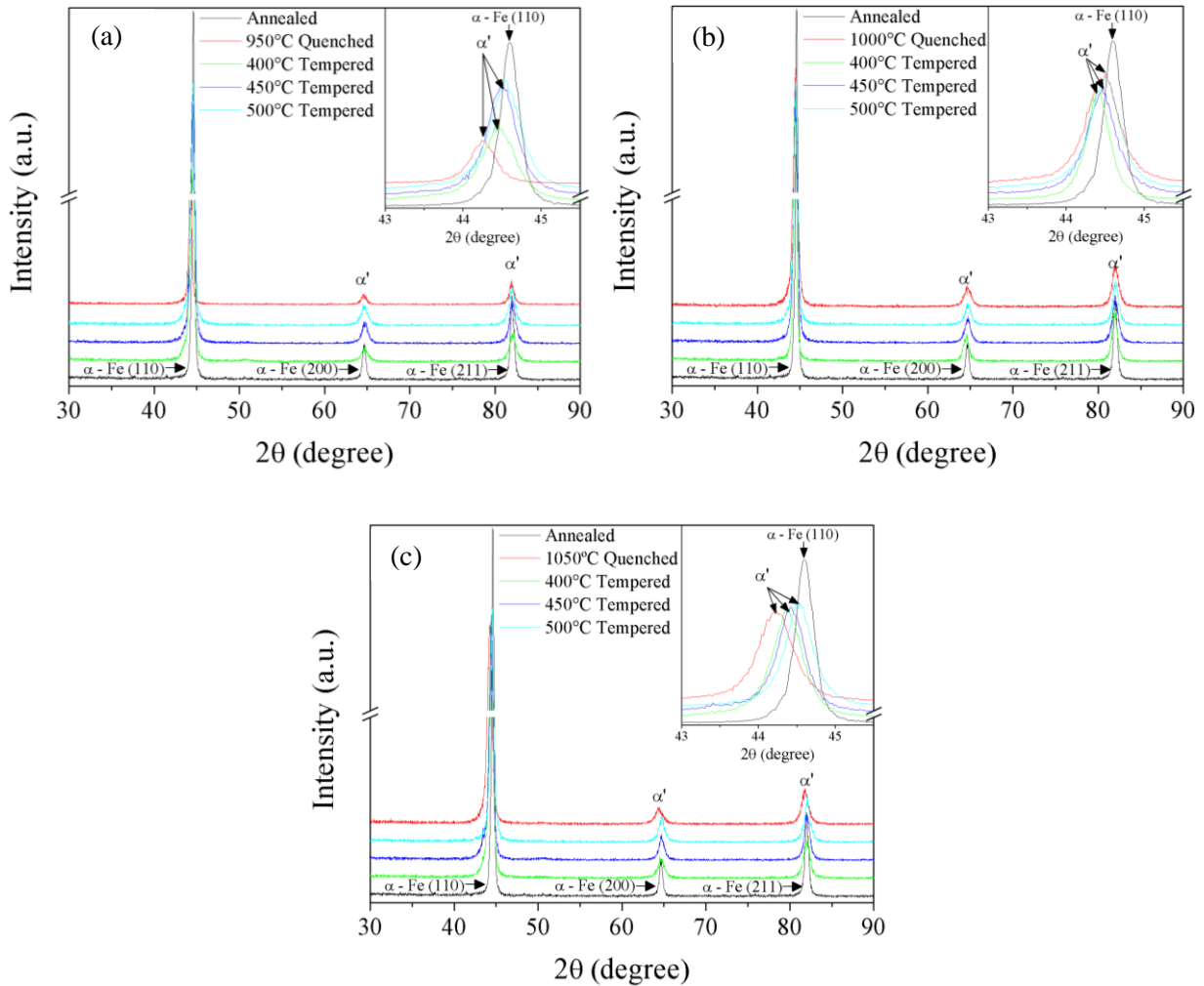


Figure 10. XRD patterns of AISI 420 steel samples tempered at 400, 450 and 500 °C for 1 h after quenched at 950 (a), 1000 (b) and 1050 °C (c).

In the Figure 10 the micrograph of 400-500°C tempered samples can be viewed. It appears that this comprises a tempered martensitic matrix. As for the micrographs presented above, the dark spots visualized in the microstructures correspond to localized corrosion attack, most attacked due to the Cr solid solution reduction, caused by the carbided precipitation. It is also observed that the amount of these dark spots decreased with increasing austenitizing temperature, and increases with the tempering temperature increase. In the first case, the smaller amount is justified because of the higher austenitizing temperature cause greater dissolution of carbides. In the second case, the temperature has the opposite effect, it causes a greater increase of the carbides nucleation, growth and coarsening. According ⁽⁶⁾, after tempering the AISI 420 steel corrosion resistance decreases due to precipitation of chromium carbides.

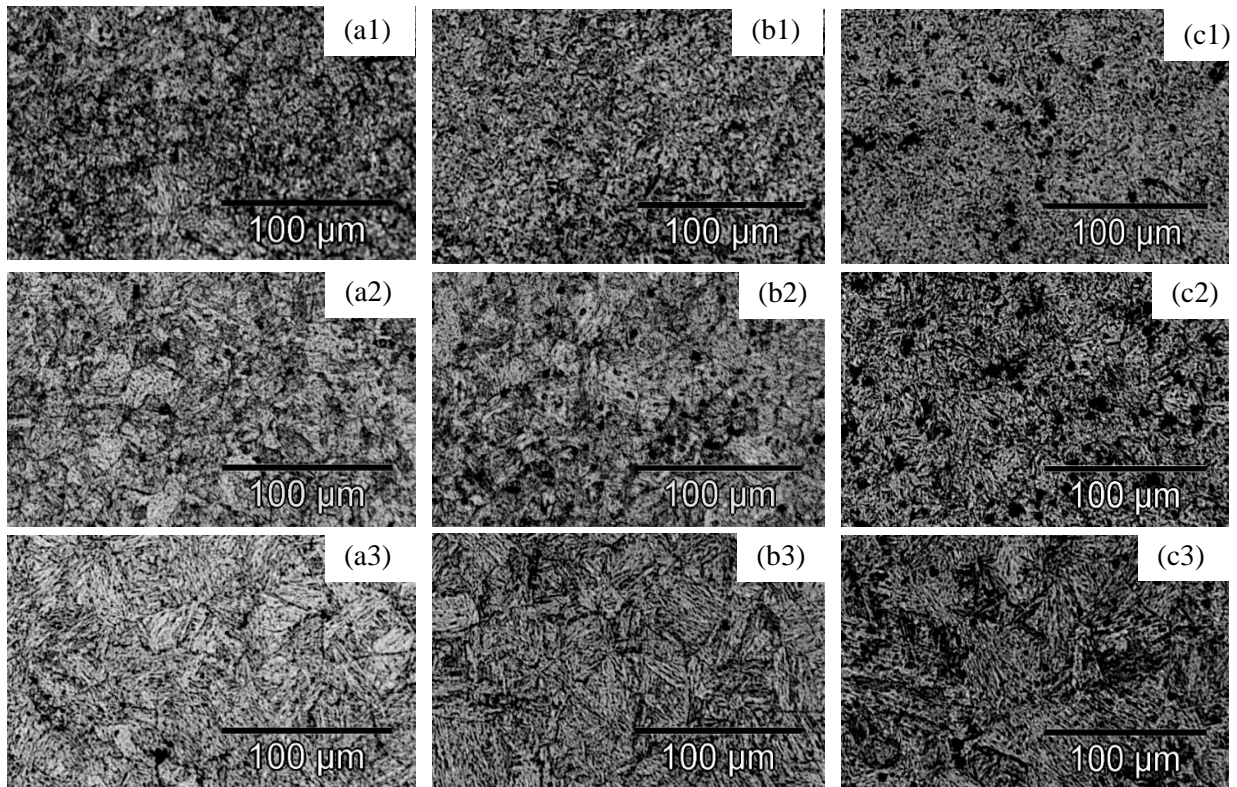


Figure 11. Microstructure of AISI 420 steel samples austenitized at 950 (a), 1000 (b) and 1050°C (c) for 0.5 h and oil quenched.

CONCLUSIONS

The effect of heat treatment parameters on the properties of AISI 420 steel have been studied and the following conclusions were taken:

- In the annealed state, the AISI 420 steel microstructure is composed by a ferritic matrix and a dispersion of $M_{23}C_6$ carbides. After austenitizing, occurs the partial dissolution of these carbides, and this phenomenon is responsible for increasing the martensite hardness with increasing austenitizing temperature. This chromium carbides solubilization increases the amount of Cr atoms dissolved in matrix causing the high corrosion resistance to austenitizing temperatures around 1050 °C;
- AISI 420 steel tempering in the temperature range of 400 to 500 ° C causes a decrease in their hardness and corrosion resistance.

ACKNOWLEDGEMENTS

This work was supported by CNPq, CAPES-COFECUB and *Programa Interdisciplinar de Petróleo e Gás Natural da UFPR* (PRH24). The authors also wish to express their thanks to the Laboratory of X-ray Optics and Instrumentation – LORXI, from the *Universidade Federal do Paraná (UFPR)* by the use of the X-ray diffraction equipment.

REFERENCES

1. ION, J.C., MOISIO, T. Laser surface modification of a 13.5% Cr, 0.6% C steel. *Journal of Materials Science*, v. 26, pp. 43-48, 1991.
2. MENG, F., TAGASHIRA, K., AZUMA, R. SOHM, H. Role of Eta-carbide Precipitations in the Wear Resistance Improvements of Fe-12Cr-Mo-V-1.4C Tool Steel by Cryogenic Treatment. *ISIJ International*, v. 34(2), pp. 205-210, 1994.
3. DUBEY, J.S., WADEKAR, S.L., CHAKRAVARTTY, J.K. Elevated temperature fracture toughness of AISI 403 martensitic stainless steel. *Journal of Nuclear Materials*, v. 254, pp. 271–274, 1998.
4. LIPPOLD C. J., DAMIAN K. J. *Welding Metallurgy and Weldability of Stainless Steels*. Canada. John Wiley & Sons, Inc., Hoboken. 2005
5. ANDRÉS, C.G., CARUANA, G., ALVAREZ, L.F. Control of $M_{23}C_6$ carbides in 0.45C–13Cr martensitic stainless steel by means of three representative heat treatment parameters. *Materials Science and Engineering: A*, v. 241 (1-2), pp. 211-215, 1998.
6. ISFAHANY, N.A., SAGHAFIAN, H., BORHANI, G. The effect of heat treatment on mechanical properties and corrosion behavior of AISI420 martensitic stainless steel. *Journal of Alloys and Compounds*, v. 509, p. 3931-3936, 2011.
7. CANDELÁRIA, A.F., PINEDO, C.E. Influence of the heat treatment on the corrosion resistance of the martensitic stainless steel type AISI 420. *Journal of Materials Science Letters*, v. 22, p. 1151 – 1153, 2003.
8. ATLAS ZUR WÄRMEBEHANDLUNG DER STÄHLE. v. 1, Verlag Stahleisen mbH, Dusseldorf, Germany, 1954.
9. KRAUSS, G. *Steels: Heat Treatment and Processing Principles*, Ed. ASM International, Fifth printing, 1997.
10. PINEDO, C.E. Estudo Morfológico e Cinético da Nitretação por Plasma Pulsado do aço Inoxidável Martensítico AISI 420. Ph.D. Thesis, Energetic and Nuclear Research Institute — São Paulo University, São Paulo, SP, Brazil, 2000 (in Portuguese). (accessible online in: http://pelicano.ipen.br/PosG30/TextoCompleto/Carlos%20Eduardo%20Pinedo_D.pdf, accessed in January 07, 2014).